Modeling cardiorespiratory interaction during human sleep with complex networks

Xi Long, Pedro Fonseca, Ronald M. Aarts, Reinder Haakma, and Jérôme Foussier

---

Articles you may be interested in

A set of 4D pediatric XCAT reference phantoms for multimodality research
Med. Phys. **41**, 033701 (2014); 10.1118/1.4864238

A technique for estimating 4D-CBCT using prior knowledge and limited-angle projections
Med. Phys. **40**, 121701 (2013); 10.1118/1.4825097

Towards a porous media model of the human lung
AIP Conf. Proc. **1453**, 69 (2012); 10.1063/1.4711155

Fractal variability: An emergent property of complex dissipative systems
Chaos **22**, 013108 (2012); 10.1063/1.3675622

Measurement of human heartbeat and respiration signals using phase detection radar
Rev. Sci. Instrum. **78**, 104703 (2007); 10.1063/1.2798937

Modeling cardiorespiratory interaction during human sleep with complex networks

Xi Long,[1,2,a] Pedro Fonseca,[1,2] Ronald M. Aarts,[1,2] Reinder Haakma,[2] and Jérôme Foussier[3]

[1]*Department of Electrical Engineering, Eindhoven University of Technology, Den Dolech 2, 5612 AZ Eindhoven, The Netherlands*
[2]*Philips Research, Prof. Holstlaan 4, 5656 AE Eindhoven, The Netherlands*
[3]*Helmholtz-Institute for Biomedical Engineering, Rheinisch-Westfälische Technische Hochschule Aachen University, Pauwelsstraße 20, 52074 Aachen, Germany*

Human sleep comprises several stages including wake, rapid-eye-movement sleep, light sleep, and deep sleep. Cardiorespiratory activity has been shown to correlate with sleep stages due to the regulation of autonomic nervous system. Here, the cardiorespiratory interaction (CRI) during sleep is analyzed using a visibility graph (VG) method that represents the CRI time series in complex networks. We demonstrate that the dynamics of the interaction between heartbeats and respiration can be revealed by VG-based networks, whereby sleep stages can be characterized and differentiated. © 2014 AIP Publishing LLC. [http://dx.doi.org/10.1063/1.4902026]

Human sleep is considered a complex biological process with its own internal architecture expressed by sleep stages.[1,2] Sleep stages can be typically separated based on patterns observed in standard polysomnography (PSG) recordings including electroencephalography (EEG), electromyography (EMG), and electrooculography (EOG).[3,4] With PSG, sleep stages are manually scored on continuous and non-overlapping epochs (lasting 30 s each) as wake, rapid-eye-movement (REM) sleep, and several non-REM (NREM) sleep stages for adults. This is usually done by trained sleep technicians according to either the recommendations provided by Rechtschaffen and Kales (R&K)[3] or using the more recent guidelines of the American Academy of Sleep Medicine (AASM).[4] NREM sleep can be further divided into stages S1-S4 based on the R&K rules, or stages N1-N3 based on the AASM guidelines. S1 and S2 (or N1 and N2) are associated with "light sleep." S3 and S4 (or N3) correspond to slow-wave sleep or "deep sleep." For normal subjects, sleep usually starts with light sleep and then deep sleep with REM sleep following.[2] This sequence is called a sleep cycle and occurs about every 90 min, four to six times per night.[2,5]

Cardiorespiratory activity has proven different characteristics across sleep stages due to the manifestation of autonomic (sympathetic and vagal) nervous activity.[1,6,7] Recently, dynamics of heartbeats and respiration during sleep have been extensively described.[8–13] In particular, characteristics of cardiorespiratory interaction (CRI) or coupling during sleep have attracted more and more attention, since they can be used to provide means to clinically diagnose sleep-related disorders or to identify sleep stages for objective sleep assessment.[14–17] For example, Bartsch et al.[17] proposed methods based on Hilbert-Huang transform (HHT) and detrended fluctuation analysis (DFA) to quantify and analyze

cardiorespiratory phase synchronization in different sleep stages.

In recent years, exploration of a time series has been extended to a two-dimensional complex network with encoded information stored in the time series, aiming at better exploiting its dynamics or properties.[18–22] Lacasa et al.[23] proposed a nonlinear visibility graph (VG) method in order to describe a time series in a graph based on specific geometric criteria. They found that random, fractal, and periodic time series correspond to networks with exponential, scale-free, and regular characteristics, respectively, which means that VG is an adaptive method for investigating different types of time series. Some studies have analyzed human physiological activity by means of VG-based networks.[24–26] For example, heartbeat dynamics in VG-based networks have been investigated for healthy subjects and patients with congestive heart failure[24] and for subjects with meditation training.[25] In the field of sleep, it has been shown that sleep stages can also be identified using parameters extracted from EEG signals based on VG-based algorithms.[26,27]

In this Letter, we apply the VG method to build complex networks for modeling a CRI time series and to analyze its dynamics across different sleep stages for healthy subjects. To formulize the VG method, let us consider a time series with n data points $\{x_k, t_k\}_{k=1,2,\ldots,n}$. Two data points (x_i, t_i) and (x_j, t_j) are connected as vertices or nodes through an undirected edge if and only if the following rule[23] is satisfied:

$$\forall \ell \in (i,j); \quad x_\ell < x_j - (x_j - x_i)\frac{t_j - t_\ell}{t_j - t_i}. \quad (1)$$

Intuitively, this means that the two data points are connected if they are able to "see" each other (i.e., the linear interpolation between their values is always larger than the value of its corresponding data point). The time series can, therefore, be converted into a VG by applying this rule on all the data points, resulting in its associated complex network with

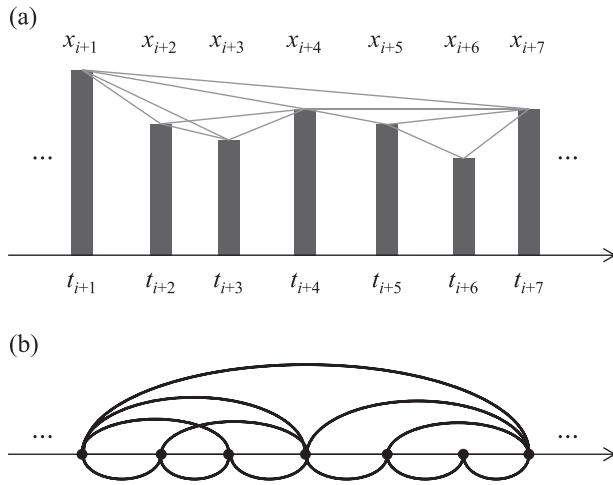[a]Electronic addresses: xi.long@philips.com and xi.long.ee@gmail.com.

(a)

(b)

FIG. 1. An example of converting (a) a time series segment with 7 data points into (b) a network using the VG method, where the respective degrees of the nodes from x_{i+1} to x_{i+7} are 4, 3, 3, 5, 3, 2, and 4.

occurrence of edges that are linked between nodes. Fig. 1 illustrates an example of converting a time series x into a VG-based network. For each node, its degree δ is defined as the number of edges attached to it, giving a heuristic indication of the network's complexity. Thus, the degree distribution of the nodes $P(\delta)$ can be used to characterize the time series.

We consider 330 overnight PSG recordings from 165 healthy subjects (87 males) from the SIESTA database.[28] Each subject spent two consecutive nights in a sleep laboratory. The subjects had an average age of 51.8 ± 19.4 yr and an average total recording time of 7.8 ± 0.5 h. According to the SIESTA study protocol, they met several criteria such as no reported symptoms of neurological, mental, medical, or cardiovascular disorders, no sleep-related disorders, no shift work, and usual bedtime between 22:00 and 24:00. The PSG recordings were visually scored on 30-s epochs by two independent raters based on the R&K rules and in case of disagreement, a consensus annotation was obtained. Here, for each 30-s epoch, the location of individual heartbeats is identified by applying the Hamilton-Tompkins R-peak detector[29] followed by a slope-based QRS complex localization method[30] on the electrocardiographic (ECG) signal with a window of 7 epochs (3.5 min) centered on the epoch of interest. This window serves the purpose of including sufficient data points to capture changes in heartbeat or RR intervals (time intervals between successive heartbeats or R peaks).[31] Afterwards, the corresponding respiratory effort at the time stamps of the heartbeats is sampled. The resulting CRI time series is then used for VG analysis. Fig. 2 illustrates an example of the computation of a CRI time series from its corresponding ECG signal and respiratory (effort) signal.

A total of 310 503 epochs (including 19.2% wake, 15.2% REM sleep, 53.5% light sleep, and 12.1% deep sleep) are analyzed in this work. Fig. 3 plots the node degree distribution of CRI, denoted as $P(\delta)$, pooled over all epochs for each sleep stage (wake, REM sleep, light sleep, and deep sleep). As illustrated, the degree distribution $P(\delta)$ for each sleep stage follows a power-law topology such that $P(\delta) \sim \delta^{-\lambda}$, in particular when the degree is large (e.g., $\delta > 4$). The power λ is shown to differ across sleep stages (wake: $\lambda = 3.7$, REM
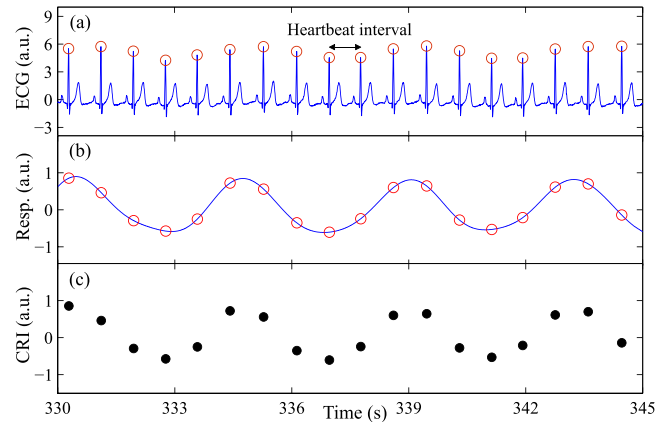

FIG. 2. An example of using (a) a 15-s ECG signal and (b) the corresponding respiratory effort signal to obtain (c) a CRI time series.

sleep: $\lambda = 3.8$, light sleep: $\lambda = 4.1$, and deep sleep: $\lambda = 4.2$). As reported in literature, a power-law topology should correspond to a scale-free dynamics,[32–34] suggesting that the CRI time series during a specific sleep stage are non-stationary and fractal.[23] In addition, we also observe that the VG-based networks of CRI for wake epochs have a higher percentage of high-degree nodes (the networks have a higher complexity) compared with other sleep stages, such as deep sleep which has the least high-degree nodes of the associated networks. A possible explanation for this is that the CRI time series is more noisy (caused by the weaker coupling between cardiac and respiratory signals) during wake, and it is more regular (due to the stronger cardiorespiratory coupling) during deep sleep when compared with the other stages.[17,20] Consequently, the CRI time series are more irregular for wake epochs while they are more regular for deep sleep epochs. The "blur" in the figure at large values of δ might be due to the presence of outliers in CRI time series caused by loose cables during measurement or body motion artifacts.

Since the degree is different between different sleep stages, it can be used to distinguish them on an epoch-by-epoch basis. For this purpose, the mean degree δ_m for each epoch (computed by averaging the degrees over the nodes
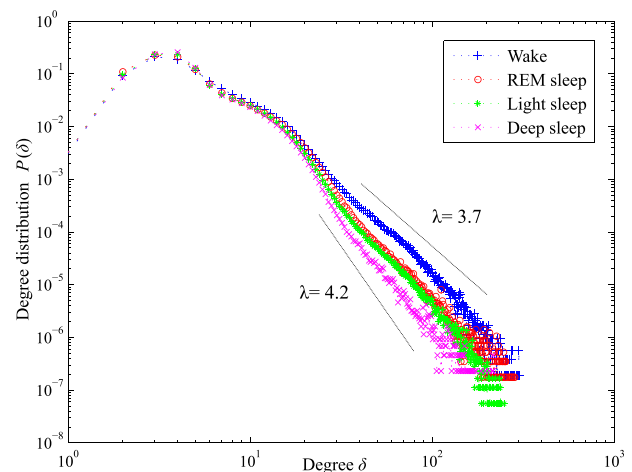

FIG. 3. Log-log plot of degree distribution $P(\delta)$ of CRI during wake, REM sleep, light sleep, and deep sleep. $P(\delta)$ follows a power-law topology when δ is larger than 4, such that $P(\delta) \sim \delta^{-\lambda}$ with λ of 3.7 for wake, 3.8 for REM sleep, 4.1 for light sleep, and 4.2 for deep sleep.
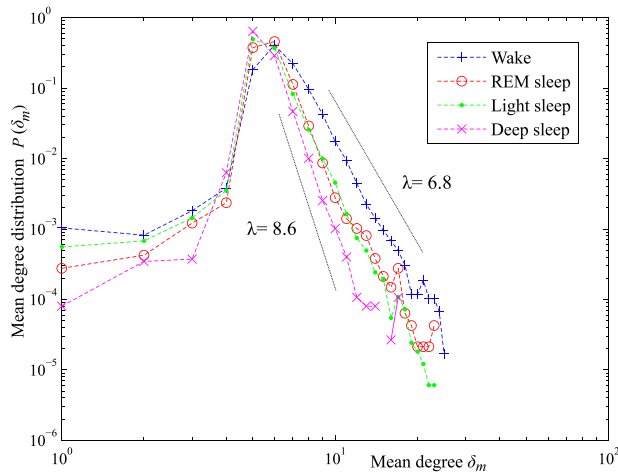
FIG. 4. Log-log plot of mean degree distribution $P(\delta_m)$ of CRI during wake, REM sleep, light sleep, and deep sleep. $P(\delta_m)$ follows a power-law $[P(\delta_m) \sim \delta_m^{-\lambda}]$ when $\lambda \geq 6$ with λ of 6.8 for wake, 7.2 for REM sleep, 8.0 for light sleep, and 8.6 for deep sleep.

FIG. 6. Degree variation δ_{sd} of the CRI time series networks (mean and standard deviation) in different sleep stages. A Mann-Whitney test shows significant differences between all pairs of sleep stages, with $p < 0.0001$.

with a window of 7 epochs centered on that epoch) can be used as a quantification of the network "complexity" of the CRI time series in VG for each epoch. Fig. 4 shows the distribution of δ_m for different sleep stages where the separations between sleep stages can be clearly observed, in particular when the mean degree is smaller than 3 or larger than 6. These results are similar to those obtained based on the analysis of EEG signals.[26] In Fig. 5, the δ_m values in different sleep stages are compared. Using a two-tailed Mann-Whitney test, δ_m is found to be significantly different between each pair of sleep stages (all with $p < 0.0001$). This means that, on average, wake epochs have the highest mean degree in the networks followed by REM sleep epochs, then by light sleep and finally by deep sleep. Moreover, if we consider the degree variation δ_{sd}, computed as the standard deviation of the node degrees in each epoch, we also find statistically significant differences between sleep stages (all with $p < 0.0001$) as illustrated in Fig. 6. The Spearman's rank correlation coefficient r between these two parameters δ_m and δ_{sd} is found to be high [r = 0.733, $p < 0.00001$; 95% confidence interval (CI) 0.730–0.736].

Another important property of a network is its assortative mixing,[35] which has been widely used to analyze many real-
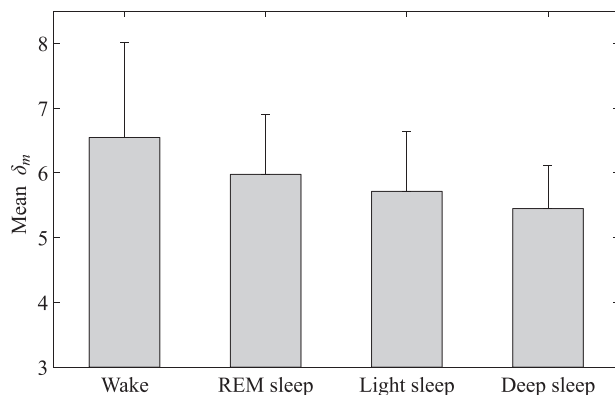
world networks such as biological,[36] neural,[37] and social networks.[38] For a node in a network, it takes the preference of its connections to high- or low-degree nodes into account. Considering a network including a total of M edges, the i-th edge connects two nodes with degree of α_i and β_i at their ends. The assortativity coefficient ζ of this network[35] is given by

$$\zeta = \frac{M^{-1}\sum_i \alpha_i \beta_i - \left[M^{-1}\sum_i \frac{1}{2}(\alpha_i + \beta_i)\right]^2}{M^{-1}\sum_i \frac{1}{2}(\alpha_i^2 + \beta_i^2) - \left[M^{-1}\sum_i \frac{1}{2}(\alpha_i + \beta_i)\right]^2}, \quad (2)$$

with ζ ranging between -1 and 1. The network is assortative if $\zeta > 0$, in which case the high-degree (or low-degree) nodes are more likely to be connected to each other than to the low-degree (or high-degree) nodes; if $\zeta = 0$, the network is randomly mixed; and if $\zeta < 0$, the network exhibits disassortativity, in which case the high-degree nodes tend to connect to the low-degree ones, and vice versa. For the CRI time series in this work, the assortativity coefficients of the associated VG-based networks in different sleep stages are shown in Fig. 7. The CRI networks in all sleep stages present assortative. In comparison with REM and NREM sleep, the CRI network has a decreased assortativity coefficient during wake, indicating that the network is more randomly mixed. Deep sleep, on the other hand, has a larger ζ compared with light sleep, possibly because the CRI time series during deep sleep exhibit a more regular pattern than light sleep. These

FIG. 5. Mean degree δ_m of the CRI time series networks (mean and standard deviation) in different sleep stages. A Mann-Whitney test shows significant differences between all pairs of sleep stages, with $p < 0.0001$.
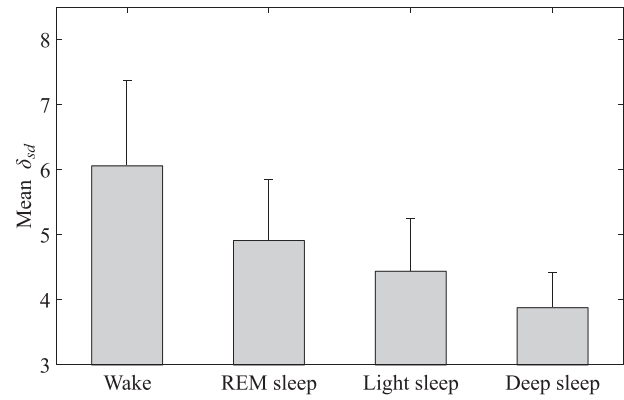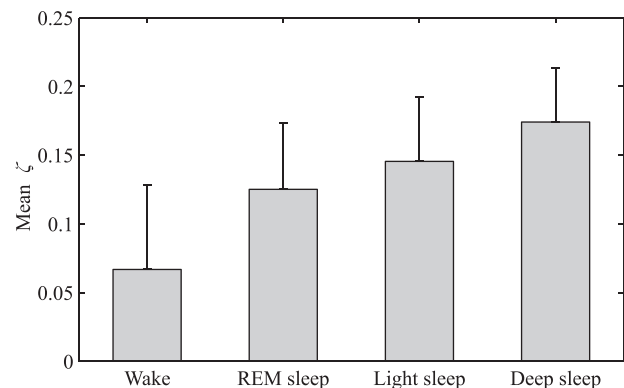

FIG. 7. Assortativity coefficient ζ of the CRI time series networks (mean and standard deviation) for different sleep stages. A Mann-Whitney test shows significant differences between all pairs of sleep stages, with $p < 0.0001$.

findings suggest that sleep stages can also be separated based on differences between the assortativity coefficients of VG-based CRI networks. It should also be noted that ζ is significantly correlated to δ_m (r $= -0.363$, $p < 0.0001$; 95% CI -0.368 to -0.358) and δ_{sd} (r $= -0.526$, $p < 0.0001$; 95% CI -0.531 to -0.522).

In conclusion, we achieve the quantification of the dynamics of cardiorespiratory interaction during sleep by converting it into complex networks using the VG method. It can be described by some important characteristics of the networks including (mean) degree and its distribution, degree variation, and assortativity coefficient. These characteristics are shown to behave differently across sleep stages. However, they are found to be correlated, possibly due to the presence of mutual information between them. Nevertheless, in practice, they offer promising features used for classifying sleep stages based on cardiorespiratory activity.

[1]V. K. Somers, M. E. Dyken, A. L. Mark, and F. M. Abboud, N. Engl. J. Med. **328**, 303–307 (1993).

[2]M. A. Carskadon and W. C. Dement, "Normal human sleep: An overview," in *Principles and Practice of Sleep Medicine*, edited by M. H. Kryger, T. Roth, and W. C. Dement (Elsevier Saunders, St. Louis, 2011), Chap. 2, pp. 16–26.

[3]E. A. Rechtschaffen and A. Kales, *A Manual of Standardized Terminology, Techniques and Scoring System for Sleep Stages of Human Subjects* (US Government Printing Office, National Institute of Health Publication, Washington, DC, 1968).

[4]C. Iber, S. Ancoli-Israel, and A. L. Chesson, *The AASM Manual for the Scoring of Sleep and Associated Events: Rules, Terminology & Technical Specifications* (American Academy of Sleep Medicine, Westchester, IL, 2007).

[5]A. N. Rama, S. C. Cho, and C. A. Kushida, "Normal human sleep," in *Sleep: A Comprehensive Handbook*, edited by T. Lee-Chiong (Wiley-Liss, New Jersey, 2006), Chap. 1, pp. 3–9.

[6]S. Akselrod, D. Gordon, F. A. Ubel, D. C. Shannon, A. C. Berger, and R. J. Cohen, Science **213**, 220–222 (1981).

[7]J. Trinder, J. Kleiman, M. Carrington, S. Smith, S. Breen, N. Tan, and Y. Kim, J. Sleep Res. **10**, 253–264 (2001).

[8]T. Penzel, J. W. Kantelhardt, C. C. Lo, K. Voigt, and C. Vogelmeier, Neuropsychopharmacology **28**, S48–53 (2003).

[9]A. Bunde, S. Havlin, J. W. Kantelhardt, T. Penzel, J. H. Peter, and K. Voigt, Phys. Rev. Lett. **85**, 3736–3739 (2000).

[10]C. K. Peng, J. Mietus, J. M. Hausdorff, S. Havlin, H. E. Stanley, and A. L. Goldberger, Phys. Rev. Lett. **70**, 1343–1346 (1993).

[11]T. Penzel, N. Wessel, M. Riedl, J. W. Kantelhardt, S. Rostig, M. Glos, A. Suhrbier, H. Malberg, and I. Fietze, Chaos **17**, 015116 (2007).

[12]X. Long, P. Fonseca, R. Haakma, R. M. Aarts, and J. Foussier, Int. J. Artif. Intell. Tools **23**, 1460002 (2014).

[13]X. Long, J. Foussier, P. Fonseca, R. Haakma, and R. M. Aarts, Biomed. Signal Process. Control **14**, 197–205 (2014).

[14]C. Schafer, M. G. Rosenblum, J. Kurths, and H. H. Abel, Nature (London) **392**, 239–240 (1998).

[15]R. Bartsch, J. W. Kantelhardt, T. Penzel, and S. Havlin, Phys. Rev. Lett. **98**, 054102 (2007).

[16]M. M. Kabir, H. Dimitri, P. Sanders, R. Antic, E. Nalivaiko, D. Abbott, and M. Baumert, Plos One **5**, e10602 (2010).

[17]R. Bartsch, A. Y. Schumann, J. W. Kantelhardt, T. Penzel, and P. Ivanov, Proc. Natl. Acad. Sci. U.S.A. **109**, 10181–10186 (2012).

[18]J. Zhang and M. Small, Phys. Rev. Lett. **96**, 238701 (2006).

[19]X. K. Xu, J. Zhang, and M. Small, Proc. Natl. Acad. Sci. U.S.A. **105**, 19601–19605 (2008).

[20]B. Luque, L. Lacasa, F. Ballesteros, and J. Luque, Phys. Rev. E **80**, 046103 (2009).

[21]R. V. Donner, Y. Zou, J. F. Donges, N. Marwan, and J. Kurths, New J. Phys. **12**, 033025 (2010).

[22]M. Ahmadlou and H. Adeli, Physica D **241**, 326–332 (2012).

[23]L. Lacasa, B. Luque, F. Ballesteros, J. Luque, and J. C. Nuño, Proc. Natl. Acad. Sci. U.S.A. **105**, 4972–4975 (2008).

[24]Z.-G. Shao, Appl. Phys. Lett. **96**, 073703 (2010).

[25]S. Jiang, C. H. Bian, X. B. Ning, and Q. D. Y. Ma, Appl. Phys. Lett. **102**, 253702 (2013).

[26]G. Zhu, Y. Li, and P. Wen, IEEE J. Biomed. Health Inf. **18**, 1813–1821 (2014).

[27]G. Zhu, Y. Li, and P. Wen, Brain Inf. LNCS **7670**, 185–195 (2012).

[28]G. Klösch, B. Kemp, T. Penzel, A. Schlogl, P. Rappelsberger, E. Trenker, G. Gruber, J. Zeitlhofer, B. Saletu, W. M. Herrmann, S. L. Himanen, D. Kunz, M. J. Barbanoj, J. Roschke, A. Varri, and G. Dorffner, IEEE Eng. Med. Biol. Mag. **20**, 51–57 (2001).

[29]P. S. Hamilton and W. J. Tompkins, IEEE Trans. Biomed. Eng. **33**, 1157–1165 (1986).

[30]P. Fonseca, J. Foussier, R. Aarts, and X. Long, SpringerPlus **3**, 376 (2014).

[31]Task Force of the European Society of Cardiology and the North American Society of Pacing and Electrophysiology, Circulation **93**, 1043–1065 (1996).

[32]R. Albert and A. L. Barabasi, Rev. Mod. Phys. **74**, 47–97 (2002).

[33]M. E. J. Newman, SIAM Rev. **45**, 167–256 (2003).

[34]S. H. Strogatz, Nature (London) **410**, 268–276 (2001).

[35]M. E. J. Newman, Phys. Rev. Lett. **89**, 208701 (2002).

[36]V. M. Eguiluz, D. R. Chialvo, G. A. Cecchi, M. Baliki, and A. V. Apkarian, Phys. Rev. Lett. **94**, 018102 (2005).

[37]S. de Franciscis, S. Johnson, and J. J. Torres, Phys. Rev. E **83**, 036114 (2011).

[38]M. E. J. Newman and J. Park, Phys. Rev. E **68**, 036122 (2003).